NEW METHOD OF CARRIER LIFETIME MEASUREMENT FOR ACCURATE POWER DEVICE SIMULATION

AKIHIRO YAHATA, YOSHIHIRO YAMAGUCHI, AKIO NAKAGAWA
AND HIROMICHI OHASHI
RESEARCH AND DEVELOPMENT CENTER, TOSHIBA CORPORATION
1, KOMUKAI TOSHIBA-CHO, SAIWAI-KU, KAWASAKI 210, JAPAN
FAX:(044)555-2074 PHONE:(044)549-2138

New method of carrier lifetime measurement is proposed for accurate power device simulation which requires the values of independent electron (τ_n) and hole (τ_p) lifetimes. Reverse recovery time and the electron beam-induced junction current of Si p^+nn^+ diodes were measured to obtain the high injection carrier lifetimes (τ_H) and τ_p, respectively. τ_n were deduced by extracting τ_p from τ_H on the basis of Shokley-Read-Hall theory. τ_n of the non-irradiated samples and samples irradiated at electron fluxes of $3x10^{13}cm^{-2}$, $5x10^{13}cm^{-2}$ and $7x10^{13}cm^{-2}$ were 3.1μs, 600ns, 360ns and 300ns, respectively. For the same samples, τ_p were 2.6μs, 72ns, 51ns and 33ns, respectively. These results indicate that τ_n/τ_p values are about 1 for non-irradiated samples and 7 to 9 for electron-irradiated samples.

INTRODUCTION

It is known that carrier lifetime plays a dominant role in determining Si device characteristics. Therefore, it is very important to evaluate carrier lifetime as well as to control it in order to improve device characteristics. To evaluate carrier lifetime, many methods including photo-conduction [1], reverse recovery time (RRT) [2], open-circuit voltage decay (OCVD) [3], scanning electron microscopy (SEM) [4], microwave reflection [5], and infrared light absorption [6], have been proposed. Even now, these various methods have not been unified into one technique, and that best suiting the device to be fabricated is generally employed. When Si power devices are fabricated, RRT and OCVD have usually been employed to evaluate carrier lifetime. Using these two methods, however, high injection conditions are attained only if the samples are of ordinary size (several square milimeters), so, it is difficult to evaluate electron (τ_n) and hole (τ_p) lifetimes separately.

τ_n/τ_p values affects very much the results of power device simulation [7]. Therefore, it is earnestly expected that τ_n and τ_p are separately obtained by experiments. In the present work, non-irradiated and electron-irradiated Si p^+nn^+ diodes, which have the simplest structure of all Si power devices, were selected as samples to determine τ_n/τ_p values. The τ_n and τ_p values were obtained separately by combining RRT with SEM for the first time.

EXPERIMENTAL

Si p^+nn^+ diodes were fabricated from magnetic-field Czochralski (MCz)-grown n-type Si substrates. The specific resistivity was 50Ω·cm. A boron-doped p^+ layer with a surface concentration of 10^{19} cm^{-3} and a phosphorous-doped n^+ layer with a surface concentration of 10^{20} cm^{-3} were obtained using conventional diffusion processes. The thicknesses of the p^+, n and n^+ in the samples for current versus voltage (I-V), DLTS and RRT experiments were 25, 50 and 170μm, respectively. Those in samples for the SEM experiments were 25, 680 and 25μm, respectively. In both RRT and SEM experiments, the n-layer carrier lifetime was measured. The n-layer carrier concentration was $10^{14}cm^{-3}$. Two kinds of Si p^+nn^+ diodes were irradiated with 10MeV electron beams with fluxes of $3x10^{13}$, $5x10^{13}$ and $7x10^{13}cm^{-2}$. Eight kinds of sample, including non-irradiated ones, were fabricated. The junction area was $8.3mm^2$.

The RRT measurement system consisted of two parts. The first part causes an electric current to flow through Si p^+nn^+ diodes. Forward current (I_F) was adjusted to a value at which the carrier density reached $10^{15}cm^{-3}$, so that high injection conditions were fulfilled. The second part applied a reverse bias (V_R) to Si p^+nn^+ diodes. The applied V_R was adjusted to give a linear decrease in current. The switching time of both parts was controlled by bipolar transistors.

The equipment employed for SEM was a Hitachi S-570. The electron beam-induced junction current (EBIC) created by irradiation of a cleaved face of a Si p^+nn^+ diode was measured with an acccelerating voltage of 20kV, a filament current of 100μA and a radiated area diameter of 100μm.

CH2987-6/91/0000-0171 $1.00 ©1991 IEEE

RESULTS AND DISCUSSION

Figure 1 shows I-V characteristics of the diodes with and without electron irradiation. In the investigated voltage range, the current at a fixed voltage increased notably upon electron irradiation. Little difference was found among the 3, 5 and 7 x 10^{13} cm^{-2} electron-irradiated samples. This current increase can be attributed to the creation of deep levels in the Si p^+nn^+ diodes.

Figure 2 shows the DLTS spectrum of the sample irradiated at 7 x 10^{13} cm^{-2}. Reverse and pulse voltages were -10 and 10V. The pulse width and rate window were 1ms and $200s^{-1}$. Two peaks were observed at 112 and 224K. It is reasonable to assume that they are electron traps in the n region, not hole traps in the p^+ region, because of the great difference in majority carrier concentration between the n and p^+ layers. We call the lower peak A and the higher peak B, as shown in the figure.

Figure 3 shows the Arrhenius plot of A and B. The values of ΔE and σ_n for A were 0.13eV and 2.8 x 10^{-18} cm^2. Those for B were 0.39eV and 3.4 x 10^{-16} cm^2.

Figure 4 shows the relationship between electron trap concentration (N_T) and electron beam flux (Φ). N_T of A was nearly equal to that of B at the constant Φ. Furthermore, the N_T values of both A and B were proportional to Φ and were described by the following equation:

$$N_T = 0.36 \times \Phi \qquad (1)$$

These results indicate that A and B have the same origin, and are induced by electron irradiation. Evwaraye and Baliga [8] also observed three electron traps with ΔE of 0.13, 0.23 and 0.41eV in 1.5MeV electron-irradiated Si p^+nn^+ diodes. They attributed them to the oxygen-vacancy pair (O-V), double negative ($[V\cdot V]^{--}$) and single negative ($[V\cdot V]^{-}$) charge states of the divacancy, respectively. They also claimed that $[V\cdot V]^{-}$ is the dominant recombination center in the electron-irradiated Si p^+nn^+ diodes. It is difficult to compare their results with ours because they did not give an Arrhenius plot in their paper. However, we speculate that our A (0.13eV) and B (0.39eV) are the same as their 0.23 and 0.41eV traps. This speculation is supported by our results which show that A and B have nearly equal concentrations and probably have the same origin (divacancy), although two questions remain. One is that their 0.13eV electron trap (O-V) is not observed in our crystals. This may be because our crystals have much lower oxygen concentrations than theirs. The other is that there are some differences in ΔE between their results and ours. In the early days of DLTS studies, correlating the sample temperature with the thermocouple was a great problem. Therefore, these ΔE differences can likely be attributed to this problem.

Figure 5 shows waveforms of RRT for the samples with thinner n-layers. (a), (b), (c) and (d) correspond to non-irradiated, $3x10^{13}cm^{-2}$, $5x10^{13}cm^{-2}$ and $7x10^{13}cm^{-2}$ irradiated samples, respectively. One vertical division represents 100mA, whereas one horizontal division reveals 100ns, respectively. Carrier lifetime (τ_H) was measured under high injection conditions in this experiment and nearly coincides with the sum of electron (τ_n) and hole (τ_p) lifetimes, according to Shockley-Read-Hall (SRH) theory [9]. The τ_H values were determined by the method proposed by Tien and Hu [10]. It is necessary in using their method that the current decreases linearly. In the cases of the samples with thicker n-layers, current did not decrease linearly and they were not employed in this experiment. Five pellets of each sample were measured. Average carrier lifetimes of (a), (b), (c) and (d) were 5.7μs, 670ns, 410ns and 330ns, respectively. The maximum scatter from the average value was 20%, 8%, 5% and 6%, respectively. The scatter was small except for the non-irradiated sample.

Figure 6 is a plot of $1/\tau_H$ versus radiation flux (Φ). Error bars show the maximum and minimum value for five pellets. $1/\tau_H$ is thought to be described by the following equation:

$$1/\tau_H = 1/\tau_H(B) + K_1 \cdot \Phi \qquad (2)$$

where $\tau_H(B)$ is τ_H of the non-irradiated sample and K_1 is a constant. The dashed line was drawn through the four points by least squares analysis, and the points barely deviate from the line. This shows that eq.(2) is fullfiled.

Figure 7 shows EBIC waveforms for the samples with thicker n-layers. Left and right sides represent n- and p-layers, respectively. The samples with thinner n-layers were not employed in the EBIC experiments because their EBIC waveforms were not triangular but trapezoidal, with the shorter parallel side of the trapezoidal waveforms coinciding with n-layer thickness. It is necessary that EBIC only comprises hole current in order to obtain hole diffusion length (L_p) and τ_p. In the case of samples with thinner n-layers, however, not only did a hole current flow from the n-layer to the p^+-layer, but also an electron current flowed from the n-layer to the n^+layer, because the n-layer was very thin and there was a difference in Fermi energy between the n

and n^+ layers. Therefore, it seems that EBIC waveforms became trapezoidal for samples with thinner n-layers. No electron current flowed materially in samples with thicker n-layers because created electrons in the n-layer disappeared untill reaching the n^+-layer. To obtain τ_p from L_p, we used the following equation:

$$L_p = (D \cdot \tau_p)^{1/2} \quad (3)$$

where D is the hole diffusion constant, assumed to be $12cm^2 \cdot sec^{-1}$. Five points on one pellet for each sample were measured. Average τ_p and the scatter from the average value were determined. The average τ_p values of (a), (b), (c) and (d) were 2.6μs, 72ns, 51ns and 33ns, respectively. The maximum scatter from the average was 50%, 36%, 18% and 21%, respectively.

Figure 8 shows $1/\tau_p$ versus Φ. Error bars represent the maximum and minimum values of the 5 points. $1/\tau_p$ is thought to be described by the following equation, as $1/\tau_H$ in eq.(2).

$$1/\tau_p = 1/\tau_p(B) + K_2 \cdot \Phi \quad (4)$$

where $\tau_p(B)$ is τ_p of the non-irradiated sample and K_2 is a constant. A dashed line was drawn through the 4 points by least squares analysis, and the 4 points hardly deviate from the dashed line. This shows that eq.(4) is fulfilled.

According to SRH theory [9], τ_H coincides with the sum of τ_n and τ_p, that is,

$$\tau_H = \tau_n + \tau_p \quad (5)$$

Using eq.(5), we obtained τ_n by extracting τ_p from τ_H, although one problem remains. We obtained τ_H for the samples with thinner n-layers and τ_p for the samples with thicker n-layers. Therefore, there is a possibility that carrier lifetime differs between samples with different n-layer thickness. However, carrier lifetime is a function of Φ, at least for irradiated samples, so we can assume that carrier lifetime is the same in samples with different n-layer thickness. Values of τ_n for (a), (b), (c) and (d) were 3.1μs, 600ns, 360ns and 300ns, respectively.

Figure 9 shows $1/\tau_n$ versus Φ. $1/\tau_n$ is also expected to be described by the following equation as in the cases of $1/\tau_H$ and $1/\tau_p$.

$$1/\tau_n = 1/\tau_n(B) + K_3 \cdot \Phi \quad (6)$$

where $\tau_n(B)$ is τ_n of the non-irradiated sample and K_3 is a constant. A dashed line was drawn through the 4 points by least squares analysis, and the 4 points lie almost on the line. This shows that eq.(6) is fulfilled, as are eqs.(2) and (4).

Table 1 summarizes the average τ_n, τ_p and τ_n/τ_p values.

SUMMARY

Electron and hole lifetimes in Si p^+nn^+ diodes were obtained separately by combining the reverse recovery time and scanning electron microscopy methods. The ratio of electron to hole lifetime for non-irradiated samples was nearly 1, whereas it was 7 to 9 for electron-irradiated samples.

References

1) L. B. Valdes, Proc. IRE, 40, 1420, 1952.
2) B. Lax and S. F. Neustadter, J. Appl. Phys., 25, 1148, 1954.
3) S. R. Lederhandler and L. G. Giacoletto, Proc. IRE, 43, 477, 1955.
4) C. Van Opdorp, R. C. Peters and M. Klerk, Appl. Phys. Lett., 24, 125, 1974.
5) H. Jacobs, A. P. Ramsa and F. A. Brand, Proc. IRE, 48, 229, 1960.
6) N. J. Harrick, J. Appl. Phys., 27, 1439, 1956.
7) A. Nakagawa, S. Nakamura and T. Shinohe, Proc. NASECODE V, 295, 1987.
8) A. O. Evwaraye and B. J. Baliga, J. Electrochem. Soc. 124, 913, 1977.
9) C. T. Sah, R. N. Noice and W. Shockley, Proc. IRE, 45, 1228, 1957.
10) B. Tien and C. Hu, IEEE Electron Device Letters, 9, 553, 1988.

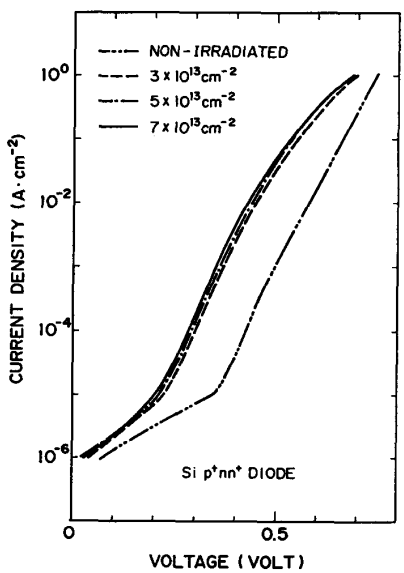

Fig.1 I-V chracteristics of diodes with and without electron irradiation.

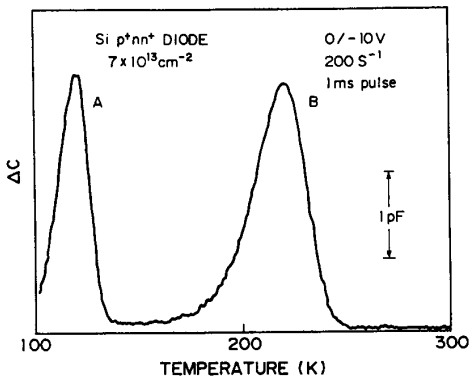

Fig.2 DLTS spectrum of the 7 x 10^{13} cm^{-2} electron -irradiated sample.

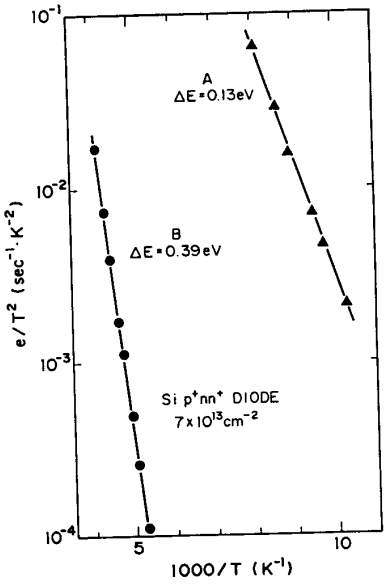

Fig.3 Arrhenius plot of A and B.

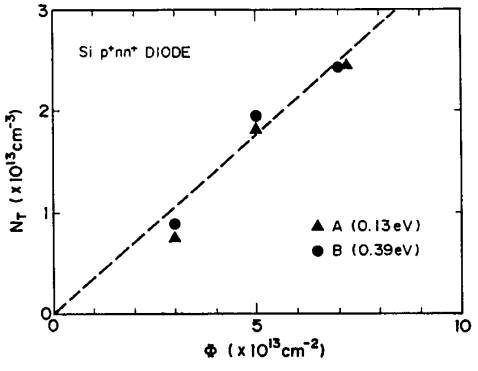

Fig.4 Relationship between electron trap. concentration (N_T) and electron beam flux (Φ)

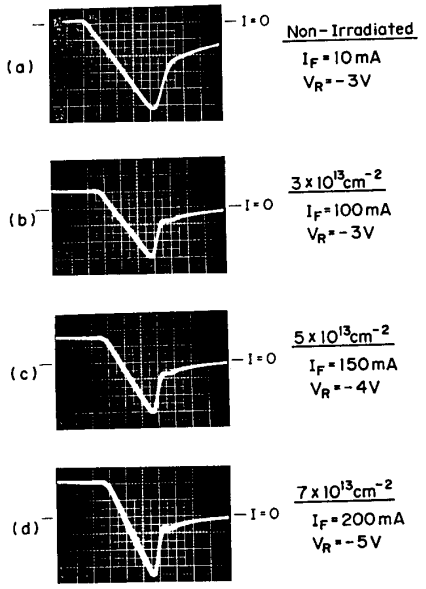

Fig.5 Waveforms of RRT of samples with thinner n -layers. (a), (b), (c) and (d) correspond to non-irradiated, 3x$10^{13}$$cm^{-2}$, 5x$10^{13}$$cm^{-2}$ and 7x$10^{13}$$cm^{-2}$ electron-irradiated samples, respectively. One vertical division represents 100mA, whereas one horizontal division reveals 100ns, respectively.

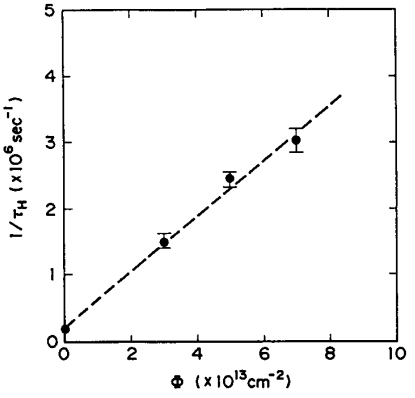

Fig.6 $1/\tau_H$ versus Φ. Error bars represent the maximum and minimum values from 5 pellets.

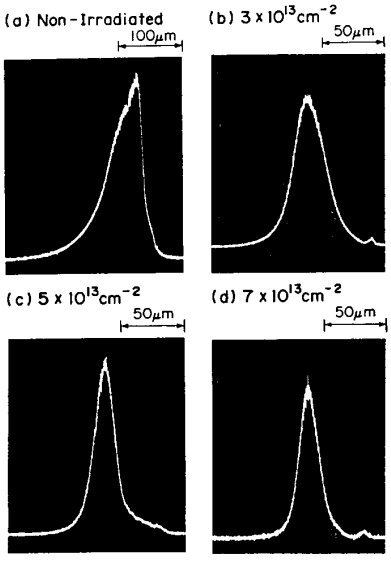

Fig.7 EBIC wavefoms for samples with thicker n -layers. (a), (b), (c) and (d) correspond to non-irradiated, $3x10^{13}cm^{-2}$, $5x10^{13}cm^{-2}$ and $7x10^{13}cm^{-2}$ electron-irradiated samples, respectively. Left and right sides represent n- and p-layers, respectively.

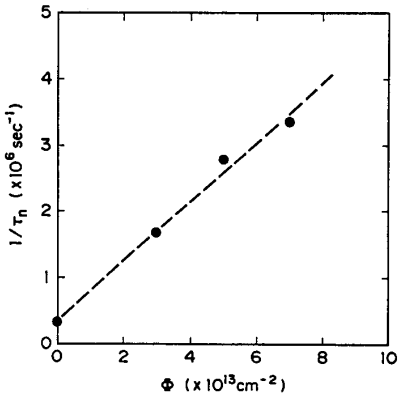

Fig. 9 $1/\tau_n$ versus Φ.

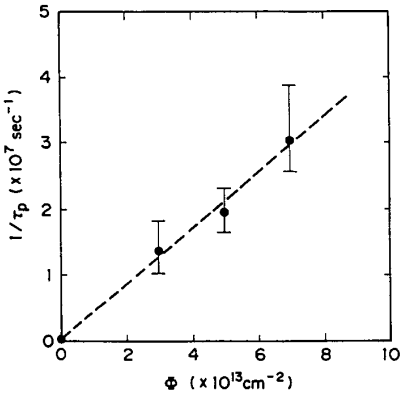

Fig.8 $1/\tau_p$ versus Φ. Error bars show the maximum and minimum values for 5 points.

Radiation Flux (cm^{-2})	τ_n (ns)	τ_p (ns)	τ_n/τ_p
Non-Irradiated	3100	2600	1.2
$3x10^{13}$	600	72	8.3
$5x10^{13}$	360	51	7.1
$7x10^{13}$	300	33	9.1

Table 1 Summary of τ_n, τ_p and τ_n/τ_p.